formed according to the manufacturer's protocol.

Experimental Protocol

Systemic and Microvascular Effects of CO. Thirty-five animals were entered for systemic MAP and HR and microvascular studies (body weight [BW] 57.5 ± 5.8 g, range 49.6–75.0 g). Blood volume (BV) was estimated at 7% of BW. Preliminary experiments determined that 10% or 20% saline top loads (n = 4 each) caused no systemic effects. Animals were divided into six groups: a) 0%, receiving 10% BV of saline (n = 4); b) 2.5%, receiving 2.5% BV of CO-saline (n = 5); c) 5%, receiving 5% BV of CO-saline (n = 4); d) 10%, receiving 10% of blood volume of CO-saline (n = 5); e) 15%, receiving 15% of blood volume of CO-saline (n = 5); and f) 20%, receiving 20% BV of CO-saline (n = 4). In the 2.5% and 5% groups, infusion volume was adjusted to 10% BV with 0.9% saline solution. Solutions were infused intravenously at the rate of 5% BV per minute. Measurements were made 10, 30, 60, and 90 mins after infusion. Four additional animals in the 20% group were observed at 120, 150, and 180 mins.

CO Effect on Cardiac Output. Ten animals were entered for this study (BW = 115.5 ± 20.9 g, range 63.0–136.0 g). Cardiac output was measured by thermodilution (10) in the 0% (n = 5) and 10% groups (n = 5). These animals had a greater BW to facilitate catheter placement.

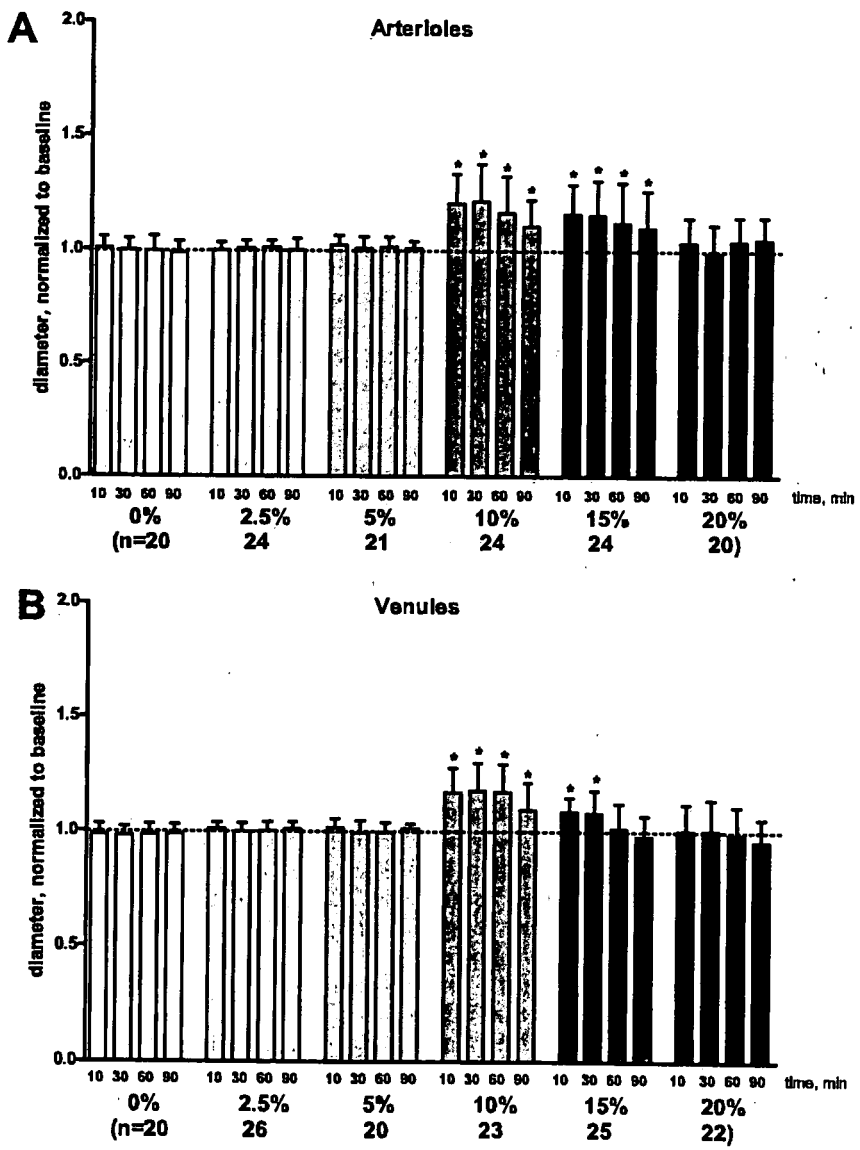

Figure 1. Changes of vessel diameters are shown normalized to baseline. Broken line represents baseline level (BL). *A*, changes of arteriolar diameter. In the 10% and 15% group, carbon monoxide (CO) caused a significant vasodilatory effect during the period of observation (*$p < .05$ vs. BL). *B*, changes of venular diameter. CO caused a significant vasodilatory effect in the 10% and 15% groups. This effect was significantly greater in the 10% group than in 15% group (†$p < .05$ vs. 15%).

Effect of NO Synthase Inhibitor L-NAME. Nine animals were entered for this study (BW = 59.2 ± 6.9 g, range 51.0–69.0 g). The effect of the nonselective NO synthase (NOS) inhibition was studied by administering intravenously 30 mg· kg^{-1} L-NAME (Sigma, St. Louis, MO) 30 mins before infusion of 10% CO-saline (11). Animals were randomly divided into two groups: a) L-NAME-s, L-NAME followed by 10% BV saline top load (n = 4); and b) L-NAME-CO, L-NAME followed by 10% BV CO-saline top load (n = 5). Measurements were made 30 mins after administration of L-NAME and 10, 30, 60, and 90 mins after the intravenous infusion of CO-saline.

Effect of sGC Inhibitor ODQ. Eighteen animals were entered for this study (BW = 61.1 ± 8.7 g, range 51.0–77.5 g). The effect of CO on the sGC-cGMP pathway was analyzed following the intravenous administration of 10 g· kg^{-1} of ODQ (Sigma) 30 mins before infusion of 10% CO-saline (12). ODQ was dissolved in dimethyl sulfoxide (DMSO) and diluted with 0.9% saline to a final DMSO concentration of about 0.04%. Animals were randomly divided into four groups: a) DMSO-s, 0.04% DMSO vehicle followed by 10% BV saline (n = 4); b) DMSO-CO, 0.04% DMSO vehicle followed by 10% BV of CO-saline (n = 5); c) ODQ-s, ODQ followed by 10% BV saline top load (n = 4); and d) ODQ-CO, ODQ followed by 10% BV of CO-saline (n = 5). Measurements were as in the L-NAME treatment experiment.

cGMP Content in the Skin Chamber Tissue. Thirty-one animals were entered for this study (BW = 65.7 ± 7.5 g, range 55.5–89.0 g). cGMP content was studied in the following groups: a) control, no treatment (n = 5); b) 10%, CO-saline (n = 5); c) 20% CO-saline (n = 4); d) L-NAME-s and 10% saline (n = 5); e) L-NAME-CO, L-NAME followed by 10% CO-saline (n = 4); f) ODQ-s, ODQ followed by 10% saline (n = 4); and g) ODQ-CO, ODQ followed by 10% BV of CO-saline (n = 4). Tissue was collected from each animal at 30 mins after either saline or CO-saline infusion.

Experimental Sequence and Data Analysis. Five studies were performed: a) dose dependency of CO-saline; b) cardiac output; c) NOS inhibition with L-NAME; d) SGC inhibition with ODQ; and g) cGMP content. After dose dependency was established, animals for each of the other studies were randomized to the different treatments groups following the scheme of Altman and Bland (13).

Results are presented as average ± SD unless otherwise noted. Data are presented as absolute values and ratios relative to baseline values. Statistical analysis was performed using one-way and paired analysis of variance when appropriate. *Post hoc* analysis was performed using Newman-Keuls' test between pairs if significance was found. All statistics were calculated by using GraphPad Prism 4.01 (GraphPad Software, San Diego, CA). Changes were considered statistically significant if $p < .05$.

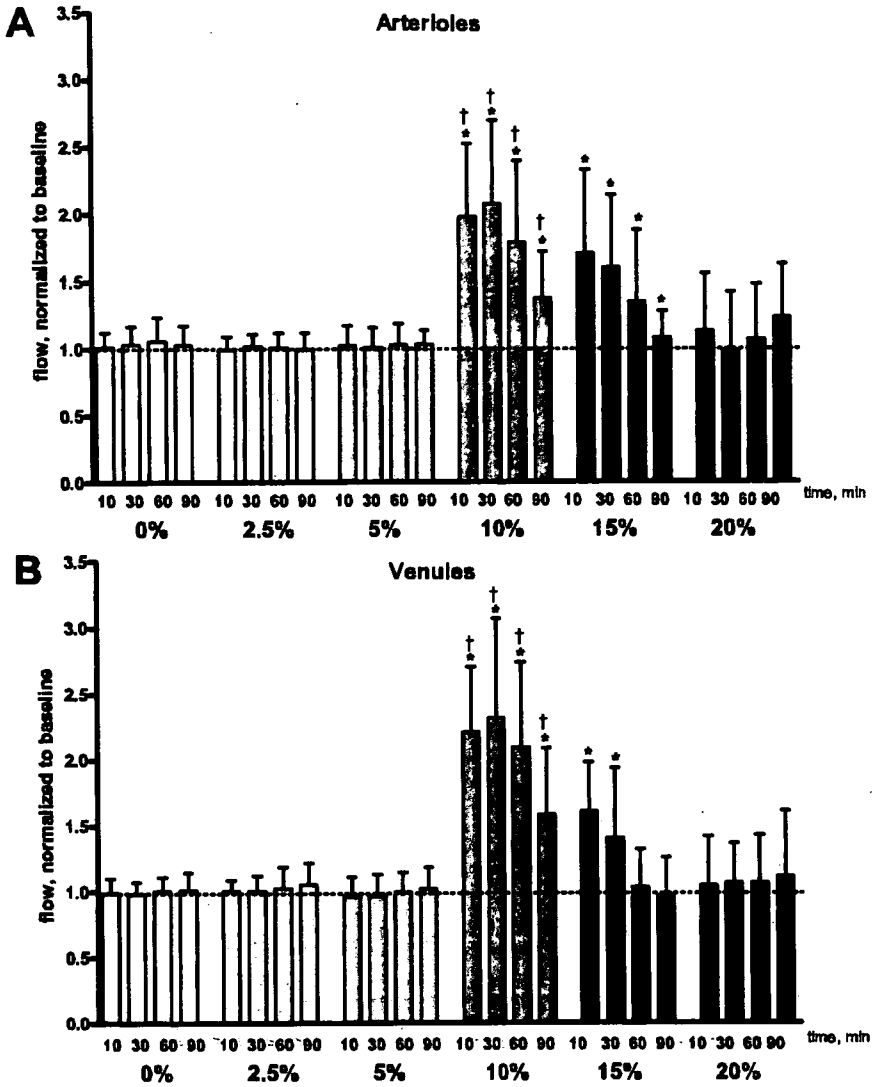

Figure 2. Calculated microvascular blood flow. Broken line represents baseline level (BL). *A*, changes of arteriolar flow. In the 10% and 15% groups, flow was increased significantly after carbon monoxide-saline injection (*$p < .05$ vs. BL). Changes of flow in the 10% group were significantly greater than those in the 15% group at 30, 60, and 90 mins (†$p < .05$ vs. 15%). *B*, changes of venular flow. In the 10% and 15% groups, flow increased significantly vs. baseline (*$p < .05$ vs. BL). Changes of flow in the 10% group were significantly greater than those in the 15% group (†$p < .05$).

RESULTS

Systemic and Microvascular Effects of CO-Saline Top Loads

MAP decreased significantly at 30 mins and 60 mins after infusion of CO-saline in the 15% group and at 90 mins in the 10% group. HR did not show significant changes (Table 1). Baseline data were no different among groups.

Saline top loads of 10% or 20% BV did not affect microhemodynamic conditions. There was a slight decrease in HR and microvascular flow; however, these effects were not statistically significant. Increase in arteriolar diameter was statistically significant after CO-saline infusion in the 10% group (maximum at 30 mins, 121%) and the 15% group (maximum at 10 mins, 116%) from baseline, lasting until the end of the observation period (Fig. 1*A*). Increase in venular diameter was statistically significant during the whole observation period in the 10% group (maximum at 30 mins, 118%) and after 10 and 30 mins in the 15% group from baseline (maximum at 10 mins, 109%)(Fig. 1*B*). The calculated upper bound concentration of CO-Hb following the 10% top load injection was 1%.

RBC velocity in both arterioles and venules increased after CO-saline infusion during the entire observation period in the 10% group and at t = 10 and 30 mins in the 15% group. Changes in the 10% group were statistically significantly greater than in the 15% group at 30 and 60 mins in arterioles and during the entire observation period in venules.

Flow increased significantly at all times in the 10% and 15% groups at 10 and 30 mins in arterioles (Fig. 2*A*) and venules (Fig. 2*B*), reaching a maximum at 30 mins. Changes of flow were significantly greater in the 10% group than in the 15% group at 30, 60, and 90 mins in arterioles and at all times in venules.

FCD increased in both the 10% and 15% groups (Fig. 3). The CO effect on FCD lasted until the end of the observation period. There were no significant differences between the 10% and 15% groups.

Since flow still increased at 90 mins in the 20% group, observations were continued to 180 mins after CO-saline infusion using another set of animals (n = 4). Vessel diameter increased significantly at 120 and 150 mins in arterioles and 120 mins in venules after CO-saline injection. RBC velocity increased at 120 mins in arterioles and 90, 120, and 150 mins in venules after CO-saline infusion. In both arterioles and venules, maximal changes of diameter and velocity were the same magnitude as those found in the 15% group. Flow increased at 120 mins in arterioles (Fig. 4*A*) and 90, 120, and 150 mins in venules (Fig. 4*B*) after CO-saline infusion. Maximal changes of flow were at 120 mins and relative values were almost the same as maximal change in the 15% group. FCD did not change during the observation period.

CO-Hb Concentration in the Systemic Circulation

CO-Hb concentration measured from arterial samples at 10, 30, 60, and 90 mins after infusion in the 10% group (n = 4) was <0.2%, the limit of resolution of the method (9, 13).

CO Effect on Cardiac Output

Animals were divided into the 0% and 10% groups. Cardiac output increased significantly at 10 mins after CO-saline injection and gradually decreased to baseline levels (Fig. 5). Cardiac index, calculated as cardiac output divided by BW, increased by 31% at 10 mins from baseline in the 10% group vs. 12% in the 0% group.

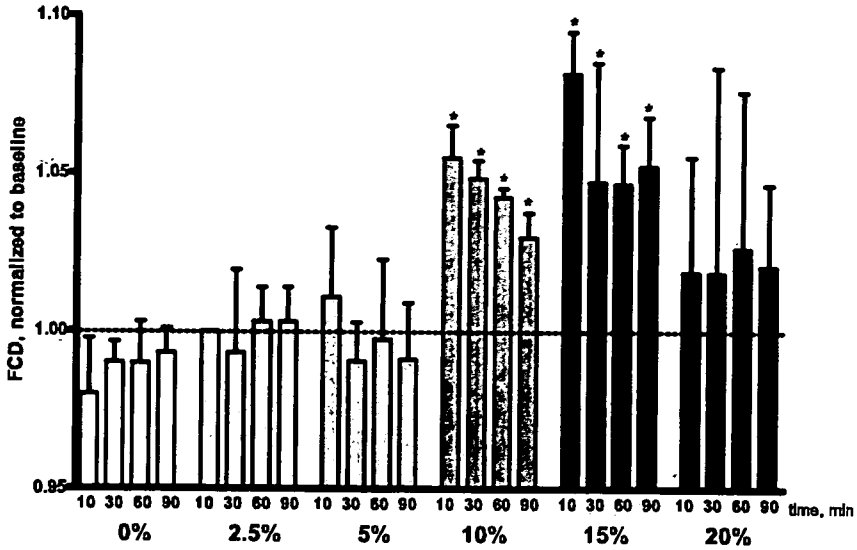

Figure 3. Functional capillary density (*FCD*) as a function of carbon monoxide (CO)-saline delivery and time. Broken line represents baseline level (BL). In the 10% and 15% groups, FCD was significantly increased after CO-saline infusion (*$p < .05$ vs. BL). There was no difference between the 10% and 15% groups.

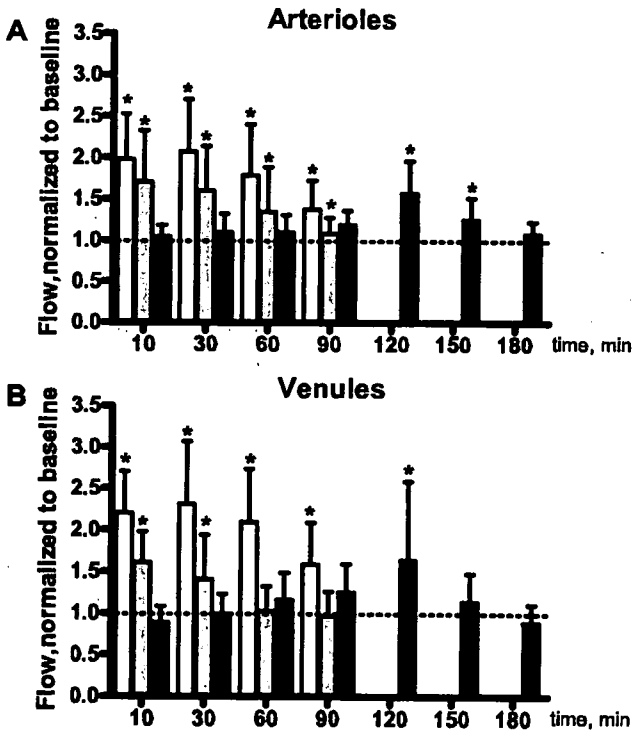

Figure 4. Changes of flow during the extended period of observation in the 20% group (*black bars*) along with 10% (*white bars*) and 15% (*light gray bars*) groups. Broken line represents baseline level (BL). Delayed increase of flow was seen in both arterioles and venules (*$p < .05$ vs. BL).

Effect of L-NAME

Administration of the nonselective NOS inhibitor L-NAME significantly increased MAP by ~20% and decreased HR by ~40%, an effect that persisted until the end of the observation period in both L-NAME-s and L-NAME-CO groups (Table 2).

In both groups, L-NAME decreased vessel diameter from baseline: arterioles (~14%) and venules (~12%). RBC velocity decreased in both groups in arterioles (~35%) and venules (~24%). In the L-NAME-CO group, arteriolar RBC velocity decreased significantly at 60 and 90 mins after CO-saline infusion. Flow was diminished by about 50% with L-NAME treatment, and 10% CO-saline could not increase flow in arterioles and venues (Fig. 6, *A* and *B*). FCD decreased nearly 30% by L-NAME treatment in both groups (Fig. 6*C*), and 10% CO-saline did not increase FCD. There were no differences between the L-NAME treated groups in any variable at any time points.

Effect of sGC Inhibitor ODQ

MAP and HR were not changed in the ODQ and DMSO-vehicle groups (Table 2). In the ODQ-CO group, RBC velocity increased at 10 and 30 mins in arterioles and at 30 mins in venules after CO-saline infusion. The DMSO vehicle had no microhemodynamic effects (Fig. 7). CO-saline increased flow significantly in both arterioles and venules at the 30-min time point after ODQ treatment. However, these changes were significantly smaller than in the 10% group (Fig. 7, *A* and 7*B*). At 30 mins after saline infusion, FCD was significantly lower than in the ODQ-treated groups (Fig. 7*C*).

cGMP Content in the Window Chamber Tissue

Hamster skin cGMP was 2470 ± 810 fmol/g in control and increased to 4860 ± 1550 fmol/g following 10% CO-saline infusion. The basal production of cGMP was not changed by L-NAME or ODQ, and cGMP content followed by 10% CO-saline infusion did not show any differences from control. L-NAME treatment significantly decreased diameter (normal groups), whereas cGMP concentration was lower than control but not significantly different (Fig. 8*A*) although the regression between diameters and for cGMP concentration was significant ($R^2 = .92$, $p < .05$) (Fig. 8*B*).

DISCUSSION

Our principal finding is that a 10% top load infusion of CO-saturated saline induced microvascular vasodilatory effects lasting up to 90 mins and increased cardiac output and capillary perfusion in the hamster window chamber model. The CO effect was concentration dependent, where 10% BV of CO-saline infusion was the most effective and lasted longer than either lower or higher concentrations. This effect was completely inhibited by L-NAME and partially by ODQ administration.

CO is known as a toxic gas, but this is a matter of dosage. At the effective dosage (10% and 15% top load), the effects in our experiments occurred within 10 mins, and increasing dosage to 20% did not produce an effect. Conversely, Kanten et al. (1) and Gutierrez et al. (2) found effects that were similar to ours after prolonged CO gas inhalation (up to several hours) or intraperitoneal 100% CO gas injection for 102 mins, reaching CO-Hb concentrations ranging from 7.5% to 58%. Therefore, it is likely that the effective dosage seen in our experiments was rapidly exceeded in experiments where CO was delivered by continuous inhalation due to the progressive accumulation of CO in blood. Since effects similar to ours were obtained with ≥10 times CO-Hb dosages by others (1, 2), it would seem that high-dosage CO involves different biochemical processes and pathways than those analyzed in the present work. Guo et al. (14) reported that CO-releasing CORM-3 compound showed effectiveness by intravenous administration when CO reached an estimated blood concentration of 20 μM, and CO-Hb in blood was 0.65% vs. control of 0.53%. They also reported that CO-Hb was virtually undetectable (<1%) until a concentration of ≥200 μM of CORM-3 was achieved *in vivo*.

CO Effects on the Systemic and Peripheral Circulation

The effects of 10% BV top load of CO-saline should be exclusively due to the presence of CO since there was no evidence of systemic or microvascular effects following a 10% BV of saline top load. MAP decreased significantly after 10% and 15% CO-saline top loads, due to the decrease of vascular resistance consequent to vasorelaxation, observed within 2 mins of injection.

Concentration-dependent effects of CO parallel similar to ours have been reported by Thorup et al (15). Repeated administration of CO was reported to lead to a decline of NO release, and higher concentration of CO inhibited endothelial NOS activity (15–17). Studies also show that CO binds to NOS, inhibiting NO production (18–22), causing vasoconstriction, and increasing blood pressure (23). These opposite observations may be explained by a dose-dependent interaction of CO and NO (24–28). Low concentration of CO causes vasoconstriction in the cerebral microcirculation (29), an effect that could be present in our model; however, 2.5% CO-saline did not show statistically significant changes in systemic and microcirculatory variables when compared with baseline and the 0% CO-saline group.

The 20% CO-saline top load caused microvascular effects similar in magnitude to those following the 15% top load but delayed by 90 mins. This shows that the CO effect on microvessels was maximized at the 10–15% concentration range, and if this range was exceeded, effects began when diffusion decreased concentration of CO.

The addition of CO to the circulating blood provides an additional stimulus to the production of NO, the principal factor in causing vasodilation. However, this mechanism is operational until the concentration of CO inhibits NO production, at which point the vasodilatory stimulus subsides. Our results suggest that once CO inhibits NO production in the endothelium, the recovery process is slow and does not take place during our experiments.

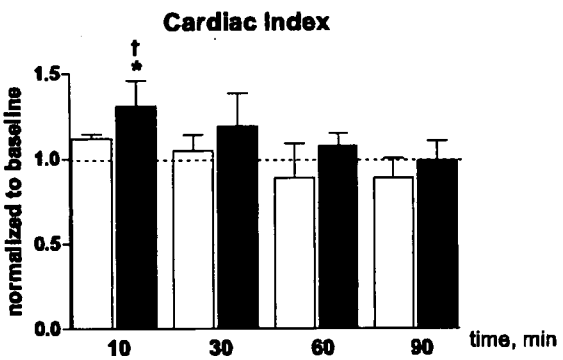

Figure 5. Cardiac index (CI) normalized to baseline in 0% carbon monoxide (CO) (*white bars*) and 10% CO (*black bars*). Broken line represents baseline level (BL). CI was significantly increased at 10 mins after CO-saline infusion (*$p < .05$ vs. BL; †$p < .05$ vs. 0%).

Table 2. Mean arterial pressure (MAP) and heart rate (HR) in L-NAME and 1H-[1,2,4]oxadiazole[4,3-a]quinoxqalin-1-one (ODQ) treatment groups

	No.	BL	Inhibitor	10 Mins	30 Mins	60 Mins	90 Mins
MAP, mm Hg							
10% CO	5	117 ± 8		117 ± 6	115 ± 9	112 ± 5	109 ± 4
L-NAME	4	110 ± 2	132 ± 7[a]	132 ± 6[a,b]	133 ± 5[a,b]	136 ± 3[a,b]	132 ± 8[a,b]
L-NAME-CO	5	115 ± 8	141 ± 5[a]	144 ± 9[a,b]	143 ± 4[a,b]	143 ± 7[a,b]	142 ± 11[a,b]
DMSO	4	106 ± 9	105 ± 10	106 ± 9	106 ± 10	106 ± 6	105 ± 8
DMSO-CO	5	106 ± 8	104 ± 6	105 ± 8	103 ± 10	106 ± 10	106 ± 10
ODQ	4	103 ± 4	103 ± 3	100 ± 3	99 ± 4	100 ± 3	98 ± 3
ODQ-CO	5	97 ± 3	96 ± 6	97 ± 6	95 ± 5	96 ± 4	95 ± 6
HR, beats/min							
10% CO	5	449 ± 27		427 ± 32	436 ± 31	432 ± 32	412 ± 52
L-NAME	4	451 ± 32	283 ± 54[a]	256 ± 81[a,b]	242 ± 67[a,b]	243 ± 54[a,b]	249 ± 47[a,b]
L-NAME-CO	5	407 ± 26	260 ± 52[a]	266 ± 47[a,b]	289 ± 62[a,b]	252 ± 38[a,b]	253 ± 23[a,b]
DMSO	4	416 ± 22	422 ± 28	409 ± 36	410 ± 16	415 ± 21	412 ± 18
DMSO-CO	5	427 ± 21	422 ± 20	425 ± 27	425 ± 17	427 ± 27	419 ± 21
ODQ	4	400 ± 19	408 ± 32	395 ± 11	403 ± 41	408 ± 18	413 ± 19
ODQ-CO	5	432 ± 28	411 ± 31	411 ± 22	427 ± 25	399 ± 37	419 ± 11

BL, baseline; CO, carbon monoxide; 10% CO, top load of 10% blood volume of CO saturated saline; DMSO, dimethyl sulfoxide.
[a]$p < .05$ vs. baseline; [b]$p < .05$ vs. 10% top load.

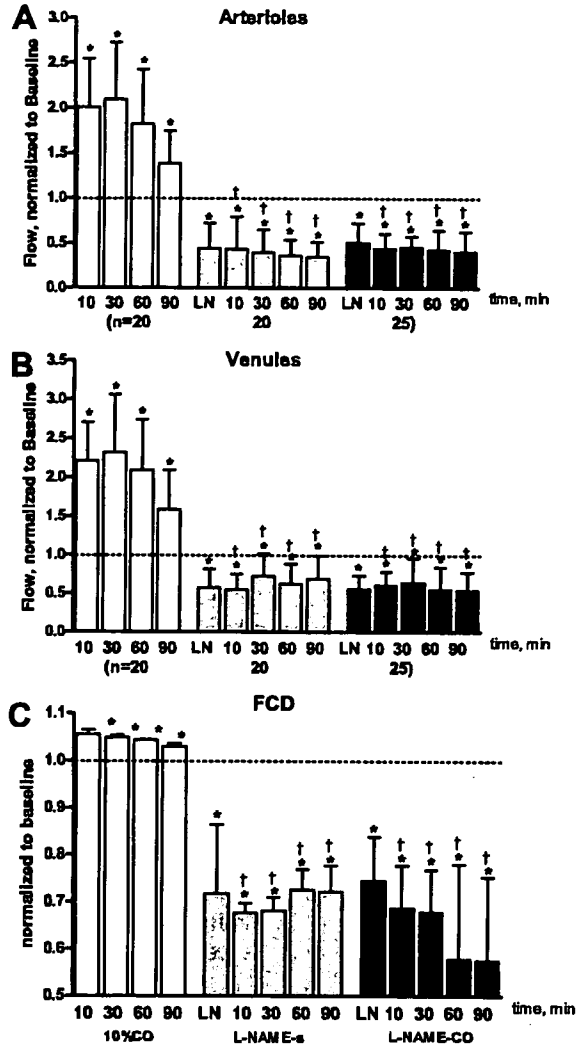

Figure 6. Changes of flow and functional capillary density (*FCD*) after L-NAME treatment (30 mg/kg^{-1}) in 10% carbon monoxide (*CO; white bars*), L-NAME followed by 10% blood volume saline top load (*L-NAME-s, gray bars*), and L-NAME followed by 10% blood volume CO-saline top load (*L-NAME-CO, black bars*). Broken line represents baseline level (BL). *A*, changes of arteriolar flow. Flow was decreased after L-NAME treatment; 10% CO-saline did not elicit the effects found in untreated hamsters (*$p < .05$ vs. BL, †$p < .05$ vs. CO-saline). *B*, changes of venular flow after L-NAME treatment. Flow was decreased after L-NAME treatment; 10% CO-saline did not elicit the effects (*$p < .05$ vs. BL, †$p < .05$ vs. CO-saline). *C*, changes of FCD after L-NAME treatment. FCD was decreased after L-NAME treatment; 10% CO-saline did not improve FCD (*$p < .05$ vs. BL, †$p < .05$ vs. CO-saline).

CO Effect on Cardiac Output

CO increased cardiac output by 30% and flow in the window chamber by 100% (at 10% top load), indicating that not all tissues and organs responded uniformly to this stimulus. The mechanism responsible for this effect is not related to the activation of cGMP by CO, which has a negative inotropic effect on the heart. The principal factor increasing cardiac output should be afterload reduction resulting from vasodilation. An additional mechanism could be activation of K_{ATP} channels, which can increase cardiac output after CO infusion (30, 31). Finally, microcirculatory effects may also take place in the heart muscle, improving cardiac perfusion and contractility.

Effect of L-NAME and ODQ

The vasodilatory effect should be due to CO stimulating sGC (32) and increasing cGMP in vascular smooth muscle (33, 34) similarly to NO. NO can enhance activity of cGMP by a factor of 200–400, whereas CO has a maximal three-fold effect (35). Consequently, the CO effect on vasorelaxation is much smaller and about one thousandth that of NO (36); however, the effects of CO are longer lasting than those due to NO, which are in the time scale of minutes. The vasodilator effect of CO is concentration dependent and nonlinear, suggesting the presence of negative responses at the higher CO concentrations.

The vasodilatory effects of the infusion of CO-saline should share the same NO-sGC pathway as those due to endogenous CO, since pretreatment with the NOS inhibitor L-NAME and sGC inhibitor ODQ caused vasoconstriction (11, 37) and hypertension. In our study, L-NAME increased MAP and decreased HR, a result obtained also by Sakai et al. (11), whereas ODQ did not affect systemic variables in rats (38). DMSO vehicle did not affect either systemic or microvascular variables; thus, inhibition effect of CO was related to sGC inhibition by ODQ.

The most effective dosage of 10% CO-saline did not induce vasodilation after L-NAME injection and only partially after ODQ injection, suggesting that CO needs NO to cause vasodilation and that the sGC-cGMP pathway is not the only pathway causing vasodilation. cGMP independent pathways such as those associated with activating calcium-dependent K^+ channel (30, 31, 39) and the cytochrome P450-monogenase pathway (40, 41) may be involved. Also, both exogenous NO and endothelium-derived relaxing factor can cause vasodilatory effects by activating the K^+ channel without cGMP in rat aortic smooth muscle (42), although Trottier et al. (43) showed that activating cGMP independent pathway required higher concentration of NO (1–9 μM). Endothelium-derived relaxing factor acts exclusively through the cGMP pathway (43); thus, CO and NO interaction should be concentration dependent as suggested by Thoroup et al (15). CO and NO are interdependent in their regulation of vasoactivity (15, 16), and since NO production is present in the hamster window chamber (44, 45), CO is able to interfere with NO-mediated vasodilation (29). L-NAME and the sGC inhibitor ODQ abolish NO availability, rendering the activity of CO ineffective. Thus, our results are compatible with the hypothesis that CO stimulates the release of NO from an intracellular storage pool that is maintained in a dynamic state by NO generated by endothelial NOS (15).

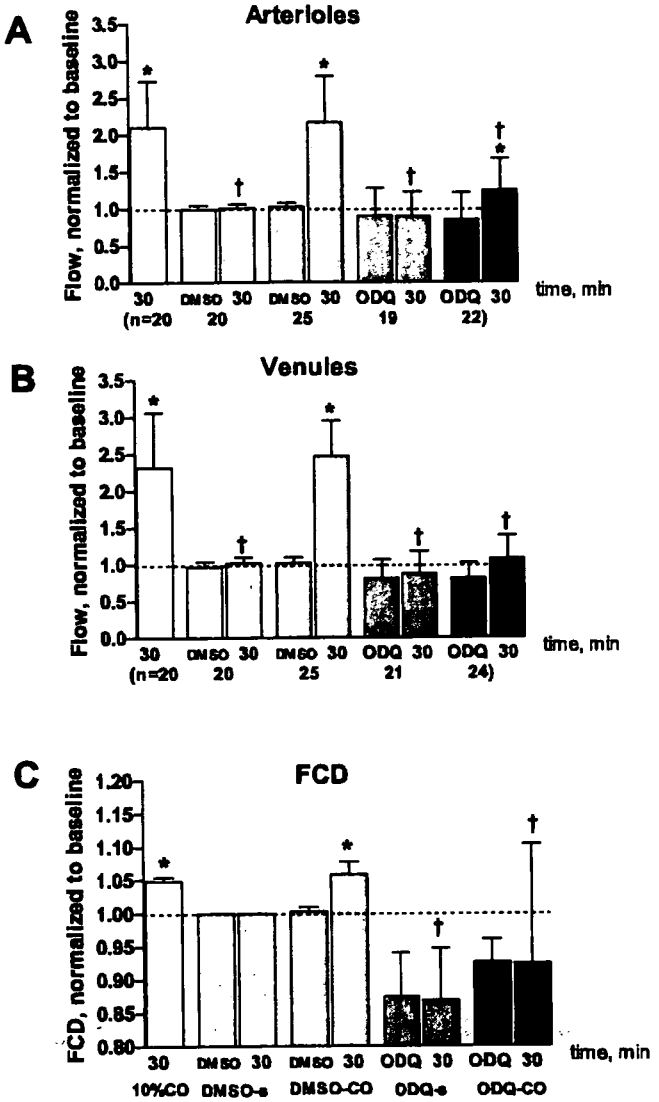

Figure 7. Microvascular flow and functional capillary density (*FCD*) after treatment with 1H-[1,2,4]oxadiazole[4,3-a]quinoxqalin-1-one (*ODQ*) (10 $\mu g \cdot kg^{-1}$) and dimethyl sulfoxide (*DMSO*) vehicle (0.04%) at 30 mins after saline or carbon monoxide (*CO*)-saline infusion: 10% CO-saline top load (*10% CO, white bars*), DMSO vehicle followed by saline top load (*DMSO-s, light gray bars*), DMSO vehicle followed by 10% CO-saline top load (*DMSO-CO, gray bars*), ODQ followed by saline top load (*ODQ-s, dark gray bars*), and ODQ followed by 10% CO-saline top load (*ODQ-CO, black bars*). Broken line represents baseline level (BL). *A*, changes of flow in arterioles. 10% CO increased flow at 30 mins after injection in arterioles (*$p < .05$ vs. BL) after DMSO and ODQ treatment; the magnitude of changes was smaller after ODQ treatment (†$p < .05$ vs. 10% CO). *B*, changes of flow in venules. 10% CO significantly increased flow in DMSO-CO group (*$p < .05$ vs. BL) but not after ODQ treatment (†$p < .05$ vs. 10% CO). *C*, changes of FCD. 0% CO increased flow at 30 mins after injection in arterioles (*$p < .05$ vs. BL) after DMSO treatment but not after ODQ treatment (†$p < .05$ vs. 10% CO).

cGMP Content in the Chamber Window Tissue

cGMP increased in the 10% CO-saline group, showing that CO stimulates sGC-cGMP. Conversely, the 20% CO-saline group could not elicit vasorelaxation at 30 mins and did not change tissue cGMP content. Therefore, under NO availability conditions, CO causes a biphasic effect on local cGMP concentration (46). These phenomena indicate that CO stimulates the release of NO from an intracellular storage pool (15), and when CO concentration is sufficient it induces the release of preformed NO bound to heme proteins (47).

It is not evident from our study whether NO release by CO originates from preexisting intracellular pools or the stimulation of endothelial NOS. However, the intracellular pool would have to be rather large to sustain 90 mins duration of dilation (at 10% top load). Furthermore, the decline of the effect at 90 mins may also reflect the decrease in CO concentration as the gas diffuses out of the circulation.

Intravenous injection of CO-saturated saline is a novel method for delivering CO. Alternatives are intraperitoneal injection of CO gas (1), inhalation (1, 2, 48, 49), and the intravenous delivery of CO-releasing molecules (50, 51). Our approach provides a quantifiable delivery of CO with rapid and long-lasting hemodynamic effects. A limitation is that volume for infusion cannot be minimized because of the solubility of CO. Intraperitoneal injection of the gas has a delayed effect, and dosage may be less predictable due to the uncertainties related to the extent of anatomical diffusion barriers between the point of injection and uptake by the blood. Inhalation requires continuous delivery of the gas for >1 hr (2), and the effect may be complicated by toxicities at the level the lung. Finally, CO delivery by CO-releasing molecules does not have the hemodynamic effects noted in the present studies (50, 51) and primarily provides tissue protection when delivered before ischemic episodes.

CONCLUSIONS

CO-saturated saline injection caused immediate vasodilation and increased blood flow in the hamster skin microcirculation, an effect that lasts as long as 90 mins. The effect is dose dependent and biphasic, since 10% BV of CO injection causes a maximal effect, whereas 2.5%, 5%, and 20% BV of CO-saline were not statistically different from baseline. This concentration of CO increased cardiac output by 30%. Pretreatment with the NOS inhibitor L-NAME completely abolished the CO effect, whereas pretreatment with the sGC inhibitor ODQ caused partial inhibition, which was confirmed by measurements of cGMP concentration in the tissues. These results indicate that CO-saline infusions are a practical method for introducing a therapeutic amount of CO into the circulation, which has a relatively long-lasting dilatory effect; however, dosage appears to be critical, since higher and lower dosages by a factor of two do not have any effect.

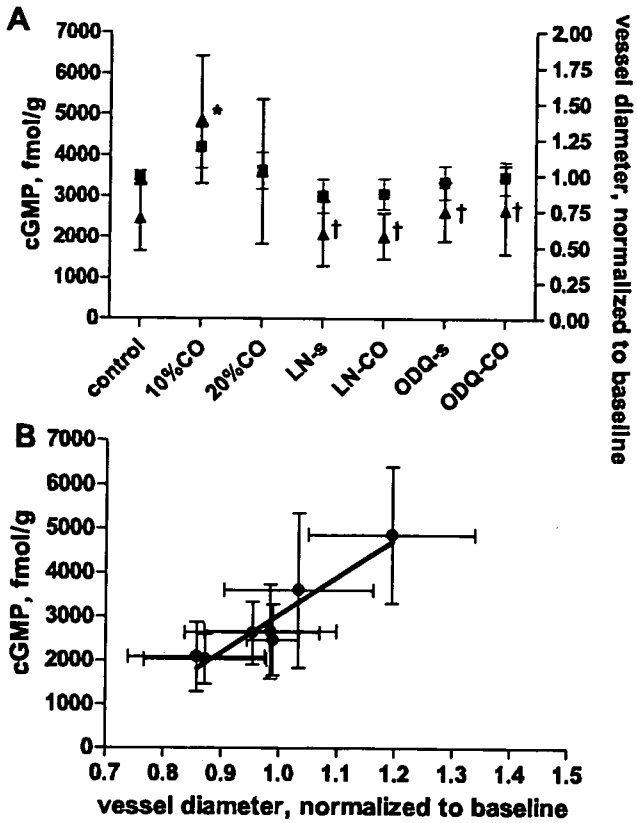

Figure 8. *A*, cyclic guanosine monophosphate (*cGMP*) concentration (*triangles*) and vessel diameter (*squares*) at 30 mins after saline or carbon monoxide (*CO*)-saline injection. cGMP in the 10% CO group was significantly higher than normal (*$p < .05$ vs. normal), L-NAME-treated, and 1H-[1,2,4]oxadiazole[4,3-a]quinoxqalin-1-one (*ODQ*)-treated groups (†$p < .05$ vs. 10% CO). *LN-s*, L-NAME followed by 10% blood volume saline top load; *LN-CO*, L-NAME followed by 10% blood volume CO-saline top load; *ODQ-s*, ODQ followed by saline top load; *ODQ-CO*, ODQ followed by 10% CO-saline top load. *B*, relation between cGMP concentration in the skin and changes of vessel diameter. There was significance between cGMP concentration and changes of diameter ($p < .05$, $R^2 = .92$).

ACKNOWLEDGMENTS

We thank F. Barra and C. Walser for their expertise in performing the animal preparations used in this work.

REFERENCES

1. Kanten WE, Penney DG, Francisco K, et al: Hemodynamic responses to acute carboxyhemoglobinemia in the rat. *Am J Physiol* 1983; 244:H320–H327
2. Gutierrez G, Rotman HH, Reid CM, et al: Comparison of canine cardiovascular response to inhaled and intraperitoneally infused CO. *J Appl Physiol* 1985; 58:558–563
3. Kerger H, Saltzman DJ, Menger MD, et al: Systemic and subcutaneous microvascular pO2 dissociation during 4-h hemorrhagic shock in conscious hamsters. *Am J Physiol* 1996; 270:H827–H836
4. Endrich B, Asaishi K, Götz A, et al: Technical report: A new chamber technique for microvascular studies in unanaesthetized hamsters. *Res Exp Med* 1980; 177:125–134
5. Intaglietta M, Silverman NR, Tompkins WR: Capillary flow velocity measurements in vivo and in situ by television methods. *Microvasc Res* 1975; 10:165–179
6. Lipowsky HH, Zweifach BW: Application of the "two-slit" photometric technique to the measurement of microvascular volumetric flow rates. *Microvasc Res* 1978; 15:93–101
7. Intaglietta M, Tompkins WR: Microvascular measurements by video image shearing and splitting. *Microvasc Res* 1973; 5:309–312
8. American College of Physicians: Practice Strategies for Elective Red Blood Cell Transfusion. Vol. 116. American College of Physicians, 1992
9. Parks J, Worth HGJ: Carboxyhemoglobin Determination by Second-Derivative Spectroscopy. *Clin Chem* 1985; 31:279–281
10. Cabrales P, Acero C, Intaglietta M, et al: Measurement of the cardiac output in small animals by thermodilution. *Microvasc Res* 2003; 66:77–82
11. Sakai H, Hara H, Tsai AG, et al: Constriction of resistance arteries determines L-NAME-induced hypertension in a conscious hamster model. *Microvasc Res* 2000; 60:21–27
12. Gimeno G, Carpentier PH, Desquand-Billiald S, et al: L-arginine and NG-nitro-L-arginine methyl ester cause macromolecule extravasation in the microcirculation of awake hamsters. *Eur J Pharmacol* 1998; 346:275–282
13. Panzali A, Signorini C, Albertini A: Improvement in lower carboxyhemoglobin range determination by second-derivative spectroscopy. *Clin Chem* 1987; 33:2311–2312
14. Guo Y, Stein AB, Wu WJ, et al: Administration of a CO-releasing molecule at the time of reperfusion reduces infarct size in vivo. *Am J Physiol Heart Circ Physiol* 2004; 286: H1649–H1653
15. Thorup C, Jones CL, Gross SS, et al: Carbon monoxide induces vasodilation and nitric oxide release but suppresses endothelial NOS. *Am J Physiol* 1999; 277:F882–F889
16. Kajimura M, Goda N, Suematsu M: Organ design for generation and reception of CO: Lessons from the liver. *Antioxid Redox Signal* 2002; 4:633–637
17. Imai T, Morita T, Shindo T, et al: Vascular smooth muscle cell-directed overexpression of heme oxygenase-1 elevates blood pressure through attenuation of nitric oxide-induced vasodilation in mice. *Circ Res* 2001; 89: 55–62
18. Klatt P, Schmidt K, Mayer B: Brain nitric oxide synthase is a haemoprotein. *Biochem J* 1992; 288:15–17
19. Matsuoka A, Stuehr DJ, Olson JS, et al: L-arginine and calmodulin regulation of the heme iron reactivity in neuronal nitric oxide synthase. *J Biol Chem* 1994; 269: 20335–20339
20. McMillan K, Masters BS: Prokaryotic expression of the heme- and flavin-binding domains of rat neuronal nitric oxide synthase as distinct polypeptides: Identification of the heme-binding proximal thiolate ligand as cysteine-415. *Biochemistry* 1995; 34: 3686–3693
21. Pufahl RA, Marletta MA: Oxidation of NG-hydroxy-L-arginine by nitric oxide synthase: evidence for the involvement of the heme in catalysis. *Biochem Biophys Res Commun* 1993; 193:963–970
22. White KA, Marletta MA: Nitric oxide synthase is a cytochrome P-450 type hemoprotein. *Biochemistry* 1992; 31:6627–6631
23. Johnson RA, Kozma F, Colombari E: Carbon monoxide: from toxin to endogenous modulator of cardiovascular functions. *Braz J Med Biol Res* 1999; 32:1–14
24. Willis D, Tomlinson A, Frederick R, et al: Modulation of heme oxygenase activity in rat brain and spleen by inhibitors and donors of nitric oxide. *Biochem Biophys Res Commun* 1995; 214:1152–1156
25. Durante W, Kroll MH, Christodoulides N, et al: Nitric oxide induces heme oxygenase-1 gene expression and carbon monoxide production in vascular smooth muscle cells. *Circ Res* 1997; 80:557–564
26. Ischiropoulos H, Beers MF, Ohnishi ST, et al: Nitric oxide production and perivascular nitration in brain after carbon monoxide poi-

soning in the rat. *J Clin Invest* 1996; 97: 2260–2267
27. Fan B, Wang J, Stuehr DJ, et al: NO synthase isozymes have distinct substrate binding sites. *Biochemistry* 1997; 36:12660–12665
28. McMillan K, Bredt DS, Hirsch DJ, et al: Cloned, expressed rat cerebellar nitric oxide synthase contains stoichiometric amounts of heme, which binds carbon monoxide. *Proc Natl Acad Sci U S A* 1992; 89:11141–11145
29. Ishikawa M, Kajimura M, Adachi T, et al: Carbon monoxide from heme oxygenase-2 Is a tonic regulator against NO-dependent vasodilatation in the adult rat cerebral microcirculation. *Circ Res* 2005; 97:e104–e114
30. Clark JE, Naughton P, Shurey S, et al: Cardioprotective actions by a water-soluble carbon monoxide-releasing molecule. *Circ Res* 2003; 93:e2–e8
31. Nishikawa Y, Stepp DW, Merkus D, et al: In vivo role of heme oxygenase in ischemic coronary vasodilation. *Am J Physiol Heart Circ Physiol* 2004; 286:H2296–H2304
32. Schmidt HH: NO, CO and OH. Endogenous soluble guanylyl cyclase-activating factors. *FEBS Lett* 1992; 307:102–107
33. Graser T, Vedernikov YP, Li DS: Study on the mechanism of carbon monoxide induced endothelium-independent relaxation in porcine coronary artery and vein. *Biomed Biochim Acta* 1990; 49:293–296
34. Marks GS, Brien JF, Nakatsu K, et al: Does carbon monoxide have a physiological function? *Trends Pharmacol Sci* 1991; 12: 185–188
35. Kharitonov VG, Sharma VS, Magde D, et al: Kinetics and equilibria of soluble guanylate cyclase ligation by CO: effect of YC-1. *Biochemistry* 1999; 38:10699–10706
36. Furchgott RF, Jothianandan D: Endothelium-dependent and -independent vasodilation involving cyclic GMP: relaxation induced by nitric oxide, carbon monoxide and light. *Blood Vessels* 1991; 28:52–61
37. Moro MA, Russel RJ, Cellek S, et al: cGMP mediates the vascular and platelet actions of nitric oxide: confirmation using an inhibitor of the soluble guanylyl cyclase. *Proc Natl Acad Sci U S A* 1996; 93:1480–1485
38. Cechova S, Pajewski TN: The soluble guanylyl cyclase inhibitor ODQ, 1H-[1,2,4]oxadiazolo[4,3-a]quinoxalin-1-one, dose-dependently reduces the threshold for isoflurane anesthesia in rats. *Anesth Analg* 2004; 99: 752–757
39. Wang R, Wu L, Wang Z: The direct effect of carbon monoxide on KCa channels in vascular smooth muscle cells. *Pflugers Arch* 1997; 434:285–291
40. Coceani F: Control of the ductus arteriosus—A new function for cytochrome P450, endothelin and nitric oxide. *Biochem Pharmacol* 1994; 48:1315–1318
41. Estabrook RW, Franklin MR, Hildebrandt AG: Factors influencing the inhibitory effect of carbon monoxide on cytochrome P-450-catalyzed mixed function oxidation reactions. *Ann N Y Acad Sci* 1970; 174:218–232
42. Bolotina VM, Najibi S, Palacino JJ, et al: Nitric oxide directly activates calcium-dependent potassium channels in vascular smooth muscle. *Nature* 1994; 368:850–853
43. Trottier G, Triggle CR, O'Neill SK, et al: Cyclic GMP-dependent and cyclic GMP-independent actions of nitric oxide on the renal afferent arteriole. *Br J Pharmacol* 1998; 125:563–569
44. Tsai AG, Acero C, Nance PR, et al: Elevated plasma viscosity in extreme hemodilution increases perivascular nitric oxide concentration and microvascular perfusion. *Am J Physiol Heart Circ Physiol* 2005; 288: H1730–H1739
45. Hangai-Hoger N, Nacharaju P, Manjula BN, et al: Microvascular effects following treatment with polyethylene glycol-albumin in lipopolysaccharide-induced endotoxemia. *Crit Care Med* 2006; 34:108–117
46. Ingi T, Cheng J, Ronnett GV: Carbon monoxide: An endogenous modulator of the nitric oxide-cyclic GMP signaling system. *Neuron* 1996; 16:835–842
47. Stamler JS, Piantadosi CA: O=O NO: It's CO. *J Clin Invest* 1996; 97:2165–2166
48. Fujimoto H, Ohno M, Ayabe S, et al: Carbon monoxide protects against cardiac ischemia-reperfusion injury in vivo via MAPK and Akt-eNOS pathways. *Arterioscler Thromb Vasc Biol* 2004; 24:1848–1853
49. Mazzola S, Forni M, Albertini M, et al: Inhaled carbon monoxide (CO) prevents lung oedema induced by endotoxic shock. *Vet Res Commun* 2004; 28(Suppl 1):209–212
50. Guo R, Gao XY, Wang W, et al: Tempol reduces reperfusion-induced arrhythmias in anaesthetized rats. *Pharmacol Res* 2005; 52: 192–198
51. Stein AB, Guo Y, Tan W, et al: Administration of a CO-releasing molecule induces late preconditioning against myocardial infarction. *J Mol Cell Cardiol* 2005; 38:127

See related article, pages 985–994

Targeting NAD(P)H Oxidase
Ets-1 Regulates p47^{phox}

Takeshi Adachi, Michiko Yamamoto, Makoto Suematsu

Reactive Oxygen Species (ROS) have been shown to modulate vascular signaling in endothelium, smooth muscle, and adventitia, regulate vascular hypertrophy, inflammation, remodeling, intracellular calcium, and disturb nitric oxide bioactivity.[1,2] Since Griendling et al discovered the activation of NAD(P)H oxidase by angiotensin II (Ang II),[3] researches have focused on the regulation of this enzyme in Ang II signaling/Ang II-induced hypertension both in vitro and in vivo. Vascular NAD(P)H oxidase consists of multiple subunits including p22^{phox}, p40^{phox}, p47^{phox}, p67^{phox}, Rac1, and unique catalytic subunits, Nox isoforms (gp91^{phox} homologue).[4] The signaling mechanisms for the rapid activation of NAD(P)H oxidase by Ang II have been identified using cultured aortic vascular smooth muscle cells (VSMCs). Ang II rapidly activates PLC to increase intracellular calcium and diacylglycerol levels, which causes the activation of protein kinase C (PKC). PKC phosphorylates p47^{phox} and releases ROS from Nox subunits. Subsequently, ROS activates cSrc, EGF-receptor, PI3-kinase, and Rac1, leading to the secondary activation of NAD(P)H oxidase to augment the intracellular ROS levels.[4] These events occur within 30 minutes in cultured VSMCs. Considering the ROS generation associated with hypertension in vivo, the latter transcriptional upregulation of NAD(P)H oxidase subunits by Ang II might be more important. Ang II upregulates the expressions of NAD(P)H oxidase subunits after more than 4 hours including p22^{phox}, Nox2 (gp91^{phox}), p47^{phox}, and p67^{phox},[5] however the mechanisms of transcriptional regulations for NAD(P)H oxidase subunits have not fully been elucidated yet.

In this issue of *Circulation Research*, Ni and colleagues identified that Ets-1 was a critical transcriptional regulator of p47^{phox} induced by Ang II in vitro and in vivo.[6] Ets-1 has been known as a proto-oncogene transcription factor to induce matrix-degradation proteins such as collagenase, plasminogen activation inhibitor-1(PAI-1), and matrix-metalloproteinases. Ets-1 can be induced by TNF-α, endothelin-1, prostanoid(s), and platelet-derived growth factor,[7–8] suggesting an implication in vascular inflammation. Indeed, this group previously reported that Ets-1 was a critical factor needed to induce cyclin-dependent kinase, PAI-I, vascular cells adhesion molecule-1, and monocyte chemoattractant protein-1 in response to Ang II. In Ets-1$^{-/-}$ mice, the vascular inflammation by Ang II infusion, which was represented by the recruitment of T cell and macrophage to vessel wall, was blunted, although hypertensive response was preserved.[9] In this article, the authors carefully seek the molecular mechanisms to regulate the expression of NAD(P)H oxidase subunits by Ets-1. The augmentation of superoxide and hydrogen peroxide (H_2O_2) generations by Ang II were markedly attenuated in aorta from Ets-1$^{-/-}$ mice or VSMCs with siRNA for Ets-1. siRNA for Ets-1 also blunted the upregulation of p47^{phox} without affecting the expression of Nox1, Nox4, Rac1, p22^{phox}, and p67^{phox} by Ang II. They used gel-shift assay, luciferase reporter assay, and chromatin immunoprecipitation assay with deletion mutant of p47^{phox} promoter, and identified the −45 Ets-1–binding promoter region as essential for the induction of p47^{phox}. They developed peptides to inhibit ETS-1 bindings (DN-Ets-1 peptides) and delivered them to the Ang II–infused mice in vivo. DN-Ets-1 peptides attenuated medial hypertrophy and aortic ROS generation without affecting hypertensive response to Ang II.

This article impacts the field of hypertension research in 3 major ways. First, the authors demonstrate the importance of p47^{phox} induction for aortic ROS generation in Ang II–induced hypertension. p47^{phox} is phosphorylated at S359/S370/S379 by PKC, which causes association with p22^{phox}. S303/S304 of p47^{phox} were also phosphorylated to augment the catalytic activity of NAD(P)H oxidase.[4] We expressed S303A/S304A mutant p47^{phox} in VSMCs to suppress the redox-sensitive signal by Ang II.[10] The posttranslational modifications of p47^{phox} by Ang II are critical for the rapid activation of NAD(P)H oxidase.

The importance of p47^{phox} expression in Ang II–induced hypertension was also shown by Landmesser and colleagues.[11] An increase in superoxide generation of aorta by Ang II was blunted in p47$^{phox-/-}$ mice but rose 3-fold in control. Hypertensive response to Ang II was modestly decreased in p47$^{phox-/-}$ mice. Consistent with these observations and the results by Ni and colleagues,[6] p47^{phox} induction is essential for aortic ROS generation and vascular inflammation in Ang II-infusion, whereas it is not required for the hypertensive response. Because Ets-1 is a critical transcriptional regulator for p47^{phox}, it is a potential therapeutic target for vascular inflammation.

Second, this study showed the importance of transcriptional regulation of the NAD(P)H oxidase. The authors clearly show the specific induction of p47^{phox} by Ets-1 without affecting the expressions of other subunits by Ang II. AP-1 was shown to regulate the expression of p67^{phox} in

---

From the Department of Biochemistry and Integrative Medical Biology, School of Medicine, Keio University, Tokyo, Japan.

Correspondence to Takeshi Adachi, MD, PhD, Department of Biochemistry and Integrative Medical Biology, School of Medicine, Keio University, Research Park 4N8, 35 Shinanomachi Shinjuku-ku, Tokyo Japan 160-8582. E-mail tadachi@sc.itc.keio.ac.jp

(*Circ Res.* **2007;101:962-964.**)

***Circulation Research* is available at http://circres.ahajournals.org**
DOI: 10.1161/CIRCRESAHA.107.164434

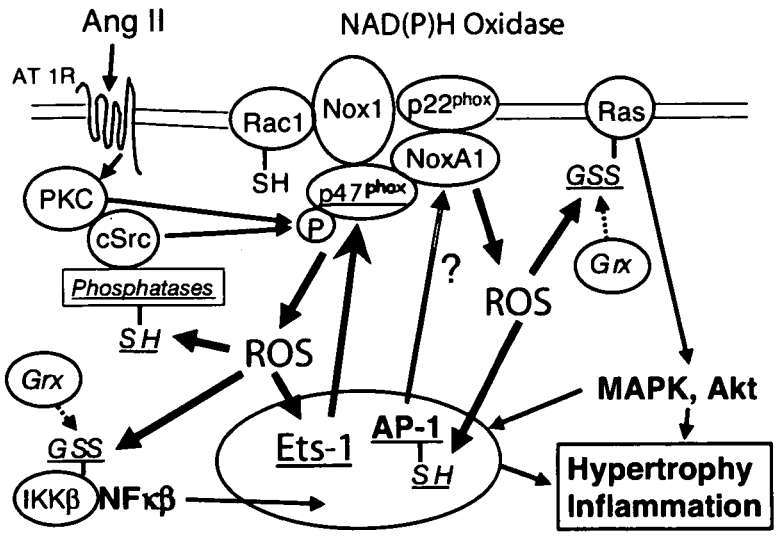

Figure. Targeting NAD(P)H oxidase. The mechanism to regulate NAD(P)H oxidase by Ang II is shown. PKC and c-Src activates NAD(P)H oxidase with the phosphorylation of $p47^{phox}$. Ets-1 upregulates $p47^{phox}$ expression. ROS from NADPH oxidase can modify thiols on the multiple target proteins and Trx/Grx reverses them. There are various strategies for targeting NAD(P)H oxidase in the system, including unique subunits, kinases/phosphatases, small GTPases, thiol-mediated regulations, and transcription factors.

monoytes,[12] however, vascular NAD(P)H oxidase may contain an alternative to $p67^{phox}$ subunit, NoxA1,[4] and the transcriptional regulation of vascular NAD(P)H oxidases are largely unknown. Stimulation of VSMCs with Ang II activates many of early genes, including AP-1 (c-fos, c-jun), NF-κβ(p50, p65), ATF/CREB, hypoxia-inducible factor-1 (HIF-1), Egr-1, STAT1, and Nrf-2.[1,13] Wilson et al[14] showed that H_2O_2 upregulated translations of Ets-1, which were mediated by the activation of Nrf-2/ARE (antioxidant response element). It is possible that the rapid activation of NADPH oxidase causes the expression of Ets-1 by redox-sensitive mechanism, which in turn induces $p47^{phox}$ for the booster effects of ROS generation by Ang II.

Redox-Sensitive Thiols Can Be Critical Targets for NAD(P)H Oxidase

Although the molecular mechanisms for the redox-sensitive signaling are not fully known, growing evidence indicates the importance of thiols modification by ROS.[15] ROS can modify the redox-sensitive thiols to sulfenylation (RSOH), sulfinylation (RSO_2H), and S-glutathiolation (RSSG). We previously found that Ang II increased ROS generation from NAD(P)H oxidase, which caused the activation of Ras via S-glutathiolation at Cys118 in VSMCs. Because many of the oncogene/transcription factors can be upregulated by the activation of Ras, the mechanism may be implicated in the ROS-mediated transcriptional regulations.[1,10] There are several other candidates for thiol-containing proteins targeted by ROS. Phosphatases have critical redox-sensitive thiols in the center of catalytic sites and the oxidation of them by ROS decreases their activity.[16] Rac1 contains a redox-sensitive thiol to modulate its function.[17] Caspase can be inhibited by S-glutathiolation,[18] and Thioredoxin (Trx) and glutaredoxin (Grx) can reverse thiol-modifications of Ras, phosphatases, and caspases.[10,15,18] Interestingly, another Trx superfamily, protein disulfide isomerase, is associated with NAD(P)H oxidase and supports ROS generation.[19] Transcriptional factors can be also regulated by ROS via redox-sensitive thiols. Cys179 on IKKβ is S-glutathiolated by ROS from Nox1, which causes NF-κβ activation.[20] ROS oxidizes the reactive thiol on Keap1 to dissociate Nrf-2, leading to the Nrf-2-transcription. In contrast, many transcription factors such as AP-1 and NF-κβ have redox-sensitive thiols in the DNA-binding sites and their modifications disturb DNA binding. The effects of ROS on transcription may differ according to the localization of ROS.[13]

Targeting NAD(P)H Oxidase for Vascular Diseases

Third, the authors used unique peptides to block Ets-1 transcription for in vivo models. DN-Ets-1 peptides contained HIV-TAT protein membrane-transduction domains to promote intracellular delivery, especially to the nucleus. In the past, Pagano and colleagues generated gp91-ds-tat peptides, which inhibited the interaction between Nox2 and $p47^{phox}$ and efficiently decreased vascular ROS from NAD(P)H oxidase.[21] Similar peptide drugs may be useful for targeting proteins related with NAD(P)H oxidase. With recent advances for understanding the regulation of NAD(P)H oxidase, we can create multiple strategies to modulate NAD(P)H oxidase activity (Figure). The AT1 receptor blocker attenuates Ang II signaling. Statin, a HMG-CoA reductase inhibitor, decreases farnysyl/geranylgeranyl pyrophosphate, leading to the suppression of Ras/Rac1.[22] Inhibition of glucose 6-phosphate dehydrogenase decreases intracellular NADPH and ROS from NAD(P)H oxidase,[23] although it may weaken the antioxidant defenses. Many of the redox-sensitive thiols and thiol-reducing enzymes (Trx/Grx/PDI) can be the downstream targets.[15] Moreover, redox-sensitive transcriptional factors can be new targets for the suppression of NAD(P)H oxidase.

Sources of Funding

The work was supported by Grants-in-Aid for Scientific Research (B:19390090) (to T.A.) and for Creative Scientific Research 17GS0419 (to T.A. and M.S.). T.A. and M.S. are core members of Global Center-of-Excellence (GCOE) for Human Metabolomics Systems Biology from MEXT. M.Y. is a research fellow supported by New Energy and Industrial Technology Development Organization.

Disclosures

None.

References

1. Griendling KK, Sorescu D, Lassegue B, Ushio-Fukai M. Modulation of protein kinase activity and gene expression by reactive oxygen species and their role in vascular physiology and pathophysiology. *Arterioscler Thromb Vasc Biol.* 2000;20:2175–2183.
2. Suzuki H, DeLano FA, Parks DA, Jamshidi N, Granger DN, Ishii H, Suematsu M, Zweifach BW, Schmid-Schoenbein GW. Xanthine oxidase activity associated with arterial blood pressure in spontaneously hypertensive rats. *Proc Natl Acad Sci U S A.* 1998;95:4754–4759.
3. Griendling KK, Minieri CA, Ollerenshaw JD, Alexander RW. Angiotensin II stimulates NADH and NADPH oxidase activity in cultured vascular smooth muscle cells. *Circ Res.* 1994;74:1141–1148.
4. Lyle AN, Griendling KK. Modulation of vascular smooth muscle signaling by reactive oxygen species. *Physiology.* 2006;21:269–280.
5. Touyz RM, Chen X, Tabet F, Yao G, He G, Quinn MT, Pagano PJ, Schiffrin EL. Expression of a functional active gp91phox-containing neutrophil-type NAD(P)H oxidase in smooth muscle cells from human resistance arteries: regulation by angiotensin II. *Circ Res.* 2002;90:1205–1213.
6. Ni W, Zhan Y, He H, Maynard E, Balschi JA, Oettgen P. Est-1 is a critical transcriptional regulator of reactive oxygen species and $p47^{phox}$ gene expression in response to angiotensin II. *Circ Res.*2007;101:985–994.
7. Naito S, Shimizu S, Maeda S, Wang J, Paul R, Fagin JA. Ets-1 is an early response gene activated by ET-1 and PDGF-BB in vascular smooth muscle cells. *Am J Physiol.* 1998;274:C472–C480.
8. Ito H, Duxbury M, Benoit E, Clancy TE, Zinner MJ, Ashley SW, Whang EE. Prostagrandin E2 enhances pancreatic cancer invasiveness through an Ets-1-dependnet induction of matrix metalloproteinase-2. *Cancer Res.* 2004;64:7439–7446.
9. Zhan Y, Brown C, Maynard E, Anshelevich A, Ni W, Ho IC, Oettgen P. Ets-1 is a critical regulator of Ang II-mediated vascular inflammation and remodeling. *J Clin Invest.* 2005;115:2508–2516.
10. Adachi T, Pimentel DR, Heibeck T, Hou X, Lee YJ, Jiang B, Ido Y, Cohen RA. S-glutathiolation of Ras mediates redox-sensitive signaling by angiotensin II in vascular smooth muscle cells. *J Biol Chem.* 2004;279:29857–29862.
11. Landmesser U, Cai H, Dikalov S, McCann L, Hwang J, Jo H, Holland SM, Harrison DG. Role of p47phox in vascular oxidative stress and hypertension caused by angiotensin II. *Hypertension.* 2002;40:511–515.
12. Gauss KA, Bunger PL, Quinn MT. Ap-1 is essential for p67(phox) promotor activity. *J Leuckoc Biol.* 2002;71:163–172.
13. Liu H, Colavitti R, Rovira II, Finkel T. Redox-dependent transcriptional Regulation. *Circ Res.* 2005;97:967–974.
14. Wilson LA, Gemin A, Espiritu R, Singh G. ets-1 is transcriptionally up-regulated by H_2O_2 via an antioxidant response element. *FASEB J.* 2005;19:2085–2087.
15. Adachi T, Schöneich C, Cohen RA. S-Glutathiolation in redox-sensitive signaling. *Drug Discov Today.* 2005;2:39–46.
16. Rhee SG, Bae YS, Lee SR, Kwon J. Hydrogen peroxide: a key messenger that modulates protein phosphorylation through cysteine oxidation. *Sci STKE.* 2000;2000:PE1.
17. Heo J, Campbell SL. Mechanism of redox-mediated guanine nucleotide exchange on redox-activate Rho GTPase. *J Biol Chem.* 2005;280:31003–31010.
18. Pan S, Berk BC. Glutathiolation regulates tumor necrosis factor-alpha-induced caspase-3 cleavage and apoptosis: key role for glutaredoxin in the death pathway. *Circ Res.* 2007;100:213–219.
19. Janiszewski M, Lopes LR, Carmo AO, Pedro MA, Brandes RP, Santos CX, Laurindo FR. Regulation of NAD(P)H oxidase by associated protein disulfide isomerase in vascular smooth muscle cells. *J Biol Chem.* 2005;280:40813–40819.
20. Reynaert NL, van der Vliet A, Guala AS, McGovern T, Hristova M, Pantano C, Heintz NH, Heim J, Ho YS, Matthews DE, Wouters EF, Janssen-Heininger YM. Dynamic redox control of NF-kappaB through glutaredoxin-regulated S-glutathionylation of inhibitory kappaB kinase beta. *Proc Natl Acad Sci U S A.* 2006;103:13086–13091.
21. Rey FE, Cifuentes ME, Kiarash A, Quinn MT, Pagano PJ. Novel competitive inhibitor of NAD(P)H oxidase assembly attenuates vascular O_2^- and systolic blood pressure in mice. *Circ Res.* 2001;89:408–414.
22. Ito M, Adachi T, Pimentel DR, Ido Y, Colucci WS. Statin inhibit beta-adrenergic receptor-stimulated apoptosis in adult rat ventricular myocyte via a Rac1-dependent mechanism. *Circulation.* 2004;110:412–418.
23. Matsui R, Xu S, Maitland KA, Hayes A, Leopold JA, Handy DE, Loscalzo J, Cohen RA. Glucose-6 phosphate dehydrogenase deficiency decreases the vascular response to angiotensin II. *Circulation.* 2005;112:257–263.

KEY WORDS: Ets-1 ■ NAD(P)H oxidase ■ Angiotensin II ■ hypertension

JPET Fast Forward. Published on January 24, 2008 as DOI:10.1124/jpet.107.132100

JPET#132100

Title Page:

Design and evaluation of S-nitrosylated human serum albumin (SNO-HSA) as a novel anticancer drug

Naohisa Katayama, Keisuke Nakajou, Hisakazu Komori, Kunitoshi Uchida, Jun-ichi Yokoe, Norikiyo Yasui, Hisashi Yamamoto, Toshiya Kai, Makoto Sato, Takenobu Nakagawa, Motohiro Takeya, Toru Maruyama, and Masaki Otagiri

Department of Biopharmaceutics (N.K., H.K., T.K., M.O.), and Department of Clinical Pharmaceutics (T.M.), Graduate school of Pharmacetical Sciences, and Department of Cell Pathology, Graduate School of Medical Sciences (T.N., and M.T.), Kumamoto University, Kumamoto, Japan; and Pharmaceutical Research Center, Nipro corporation, Shiga, Japan (N.K., K.N., K.U., J.Y., N.Y., H.Y., T.K., M.S)

Running Title Page:

NO-HSA induces tumor cell apoptosis

Address correspondence to:

Masaki Otagiri, Department of Biopharmaceutics, Graduate school of Pharmacetical Sciences, Kumamoto University, 5-1 Oe-honmachi, Kumamoto 862-0973, Japan. Tel: +81-96-371-4150, Fax: +81-96-362-7690, E-mail: otagirim@gpo.kumamoto-u.ac.jp

The number of text pages: 33

The number of tables: 1

The number of figures: 6

The number of references: 40

The number of words in the Abstract: 242

The number of words in the Introduction: 571

The number of words in the Discussion: 1461

ABBREVIATIONS: NO, nitric oxide; NO-HSA, nitrosated human serum albumin; rHSA, recombinant human serum albumin; ROS, reactive oxygen species; NO-NSAID, nitric oxide-donating non-steroidal anti-inflammatory drug; NO-ASA, nitric oxide-donating aspirin; DTPA, diethylenetriaminepentaacetic acid; HBSS, Hanks' balanced salt solution; KPB, potassium phosphate buffer; C26, murine colon 26 carcinoma; FCS, fetal calf serum; CM-H_2DCFDA, 5-(and-6)-chloromethyl-2',7'-dichlorodihydrofluorescein diacetate, acetyl ester; FITC, fluorescein isothiocyanate; HRP, Horseradish Peroxidase; TdT, terminal

deoxynucleotidyl transferase; DAB, 3,3-diaminobenzidine; Cr, serum creatinine; BUN, blood urea nitrogen; ALT, alanine aminotransferase; AST, aspartate aminotransferase; ALP, alkaline phosphatase; CD, circular dichroism; PAGE, polyacrylamide gel electrophoresis; BSA, bovine serum albumin; GSH, glutathione; GSNO, S-nitrosoglutathione; R410C, genetic variant of human serum albumin mutated at position 410.

Abstract

Recently, the cytotoxic activity of NO has been investigated for its potential use in anticancer therapies. Nitrosated human serum albumin (NO-HSA) may act as a reservoir of NO *in vivo*. However, there are no published reports regarding the effects of NO-HSA on cancer. Therefore, the present study investigated the anti-tumor activity of NO-HSA. NO-HSA was prepared by incubating HSA, which had been sulfhydrylated using iminothiolane, with isopentyl nitrite (6.64 mol NO/mol HSA). Anti-tumor activity was examined *in vitro* using murine colon 26 carcinoma (C26) cells and *in vivo* using C26 tumor-bearing mice. Exposure to NO-HSA increased the production of reactive oxygen species (ROS) in C26 cells. Flow cytometric analysis using rhodamine 123 showed that NO-HSA caused mitochondrial depolarization. Activation of caspase-3 and DNA fragmentation were observed in C26 cells after incubation with 100 μM NO-HSA for 24 h, and NO-HSA inhibited the growth of C26 cells in a concentration-dependent manner. The growth of C26 tumors in mice was significantly inhibited by administration of NO-HSA compared with saline- and HSA-treatment. Immunohistochemical analysis of tumor tissues demonstrated an increase in TUNEL-positive cells in NO-HSA-treated mice, suggesting that inhibition of tumor growth by NO-HSA was mediated through induction of apoptosis. Biochemical parameters (such as Cr, BUN, AST and ALT) showed no significant differences among the three treatment groups, indicating that NO-HSA did not cause hepatic or renal damage. These results suggest that NO-HSA has the potential for chemopreventive and/or chemotherapeutic activity with few side effects.

Introduction

Although cancer primarily arises from disorders of cell proliferation, it also may arise from disruptions in programmed cell death signaling pathways, resulting in decreased apoptosis of cancerous cells (Okada et al., 2004). Therefore, induction of apoptosis in neoplastic cells is a very effective therapy for tumor eradication (Meng et al.,2006). However, this type of chemotherapy often has negative side effects, such as transient cell cycle arrest, senescence, and autophagy. Drug delivery systems that facilitate selective apoptosis of neoplastic cells have been suggested as a way of overcoming this problem (Kaufmann et al., 2000; Kondo et al., 2005).

Nitric oxide (NO) is a unique diffusible molecular messenger that occupies a central role in mammalian pathophysiology (Brune et al., 1998). Its multiple actions include vascular smooth muscle relaxation (Moncada et al., 1986; Ignarro et al., 1989), inhibition of platelet aggregation (Azuma et al., 1986), effects on neurotransmission (Garthweite, 1991), and regulation of immune function (Marletta et al., 1988). Alternatively, under some circumstances, NO is cytotoxic (Laval et al., 1994). NO causes cellular iron losses and inhibits DNA synthesis, mitochondrial respiration, and aconitase activity in L10 hepatoma cells (Hibbs et al., 1988). In addition, NO reacts with superoxide anion (which is produced by activated macrophages and other cells), to form peroxynitrite. This byproduct of NO is a potent chemical oxidant, which alters protein function and damages DNA (Beckman et al., 1993). These effects are part of the nonspecific host defense, which facilitates killing of tumor cells and intracellular pathogens. In addition, the cytotoxicity arising from long-lasting NO generation has been attributed to induction of apoptosis (Brune et al., 1998).

Recently, the cytotoxic activity of NO has been studied to assess its therapeutic

potential in cancer treatment. NO-donating non-steroidal anti-inflammatory drugs (NO-NSAIDs), especially NO-aspirin (NO-ASA), have been investigated as promising chemopreventive agents (Fabbri et al., 2005; Kashifi et al., 2002; Williams et al., 2001). NO-ASA consists of traditional ASA to which a NO-releasing moiety is bound via a spacer. This agent induces oxidative stress by increasing intracellular peroxide and $O_2^{\cdot}$, thereby inducing apoptosis via activation of the intrinsic apoptosis pathway (Gao et al., 2005). JS-K is a pro-drug designed to release NO after reacting with glutathione S-transferase, which induces double-stranded DNA breaks, activates DNA-damage-response pathways, and induces apoptosis in human multiple myeloma cells both *in vitro* and *in vivo* (Kiziltepe et al., 2007).

Human serum albumin (HSA) is an abundant circulating protein and the nitrosated form serves as a reservoir of NO (Stamler et al., 1992). Therefore, NO-HSA is an NO donor that is currently being investigated for its potential therapeutic applications. For example, administration of NO-HSA to animals with ischemia-reperfusion injury minimizes the tissue damage that occurs after reperfusion (Semisroth et al., 2005). In a balloon-injured rabbit femoral artery model, locally delivered NO-HSA preferentially binds to sites of vessel injury and inhibits both platelet accumulation and the subsequent development of neointimal hyperplasia (Marks et al., 1995). NO-HSA also shows potent antibacterial activity and inhibits the proliferation of cultured human vascular smooth muscle cells (Ishima et al., 2007). However, there are no reports describing the effects of NO-HSA on cancer.

Accordingly, the present study evaluated the anti-tumor activity of NO bound to HSA (NO-HSA) via an S-nitrosothiol linkage using iminothiolane as a spacer. The molecular events related to induction of apoptosis by NO-HSA were studied *in vitro* and

the antitumor activity of NO-HSA was studied *in vivo* using a murine model of C26 colon carcinoma.

Methods

Chemicals

Traut's Reagent (2-imminothiolane) was purchased from Pierce Chemical Co. (Rockford, IL, USA). Isopentyl nitrite, diethylenetriaminepentaacetic acid (DTPA) and Cell Counting Kit-8 were purchased from Wako Pure Chemical Industries, Ltd. (Osaka, Japan). RPMI-1640 medium, Hanks' balanced salt solution (HBSS) and RNase A was obtained from Sigma Chemical (St Louis, MO, USA). Proteinase K was obtained from Roche Applied Science (Indianapolis, IN, USA). All other reagents used were of the highest grade available from commercial sources.

Expression and purification of recombinant human serum albumin (rHSA)

rHSA was produced using a yeast expression system as described previously (Matsushita et al., 2004). Briefly, for constructing the HSA expression vector pPIC9-HSA, native HSA coding region was incorporated into the methanol-inducible pPIC9 vector (Invitrogen Co., San Diego, CA, U.S.A.). The resulting vector was introduced into the yeast species *P. pastoris* (strain GS115) to express rHSA. Secreted rHSA was isolated from the growth medium by a combination of precipitation with 60% (w/v) $(NH_4)_2SO_4$ and purification on a Blue Sepharose CL-6B column (GE Healthcare) followed by Phenyl HP column (GE Healthcare). Isolated protein was defatted by using the charcoal procedure described by Chen (Chen, 1967), deionized, freeze-dried and then stored at -20°C until use. The resulting rHSA (treated with dithiothreitol) exhibited a single band on SDS/PAGE. Density analysis of protein bands stained with Coomassie Brilliant Blue showed that its purity was more than 97%.

Synthesis of nitroso-albumin (NO-HSA)

Terminal sulfhydryl groups were added to the HSA molecule by incubating 0.15 mM rHSA with 3 mM Traut's Reagent (2-imminothiolane) in 100 mM potassium phosphate buffer (KPB) containing 0.5 mM DTPA (pH 7.8) for 1 h at room temperature. The resultant modified rHSA then was S-nitrosylated by 3 h incubation with 15 mM isopentyl nitrite at room temperature (Figure 1). The resulting NO-HSA was concentrated, exchanged with saline using a PelliconXL filtration device (Millipore Corporation, Billerica, MA, USA), and the final concentration adjusted to 2 mM NO-HSA. The sample was stored at -80 °C until use.

Determination of S-nitrosylation efficiency

The amount of the *S*-nitroso moieties of NO-HSA was quantified using a 96-well plate. First, 20-μl aliquots of NO-HSA solution and $NaNO_2$ (standard) were incubated with 0.2 ml of 10 mM sodium acetate buffer (pH 5.5) containing 100 mM NaCl, 0.5 mM DTPA, 0.015% N-1-naphthylsthylene-diamide and 0.15% sulfanilamide with or without 0.09 mM $HgCl_2$, for 30 min at room temperature. Then, the absorbance was measured at 540 nm. The number of moles of NO per mole of HSA, was obtained by subtracting the values in the absence of $HgCl_2$ from values in the presence of $HgCl_2$; the value thus obtained, was 6.64 ± 0.54 mol NO/mol HSA.

Cellular experiments with Colon-26 (C26) cells

C26 cells, which were donated by the Institute of Development, Aging and Cancer, at Tohoku University (Sendai, Miyagi, Japan), were cultured at 37°C in RPMI 1640